Chaos-induced avoided level crossing and tunneling

Miroslaw Latka, Paolo Grigolini, and Bruce J. West
University of North Texas, P.O. Box 5368, Denton, Texas 76203
(Received 14 February 1994)

We study the quantum effect of chaos on dynamical tunneling in the driven pendulum. We analyze the avoided level crossing between the Floquet states associated with the chaotic part of the phase space and a member of the quasidegenerate doublet. As a result of the interaction, the doublet state whose Husimi distribution was initially localized on symmetric Kolmogorov-Arnold-Moser islands exchanges its structure with the chaotic state. We investigate the implications of this kind of avoided crossing on the quantum dynamics of a wave packet initially centered on one of the symmetric islands.

PACS number(s): 03.65.−w, 05.45.+b, 73.40.Gk

I. INTRODUCTION

Despite significant recent progress, relatively little is known about the effects of chaos on a purely quantum mechanical process such as tunneling. Herein we adopt a broader definition of tunneling which comprises not only the conventional penetration of a classically insurmountable potential barrier but also the quantum motion between classically disconnected phase space nonlinear resonances [Kolmogorov-Arnold-Moser (KAM) islands]. The latter phenomenon was investigated by Davis and Heller as early as 1981 and is frequently referred to as dynamical tunneling [1].

The interplay between chaos and tunneling was the subject of the recent work by Lin and Ballentine [2, 3], who investigated a monochromatically driven particle in a double-well potential. The Poincaré surface of section of this system for a particular choice of model parameters has a small regular island in each well immersed in a chaotic sea, which extends over both wells. Lin and Ballentine show numerically that a wave packet initially centered on one stability island tunnels into the other one. The tunneling between the classical phase space structures retains its coherent, oscillatory nature despite the fact that the wave packet is not completely enclosed by the KAM surfaces. The driven tunneling phenomenon has a rate 10^4 faster than that for the undriven case. Peres [4] pointed out that the observed tunneling is due to a dynamical symmetry of the Hamiltonian, which remains invariant under combined spatial reflection and time translation. Consequently the eigenfunctions of the corresponding Floquet operator may be classified into even and odd states with respect to a generalized parity operator. In further investigations Plata and Llorente [5] demonstrated that the tunneling rate is determined by the splitting of a pair of Floquet states localized on two stability regions. Symmetric and antisymmetric combinations of these states yield packets initially localized in each well which in the course of time oscillate between the stability regions. Grossman *et al.* [6–9] studied the driven double well model with different values of the frequency and amplitude of the perturbation and showed that the external field can also decrease the tunneling rate and with the appropriate choice of model parameters it is possible to even suppress the tunneling altogether. The total inhibition of the tunneling occurs at the exact crossing of the even and odd Floquet states. Utermann *et al.* [10] found a very strong correlation between the tunnel splitting and the overlap of the Husimi distribution of the doublet states with the chaotic layer.

The problem of phase space tunneling has been studied for many quite diverse physical systems. For example, Roncaglia *et al.* [11], using the kicked Harper model in the regime of weak chaos, examined the dependence of the splitting of the nearly degenerate doublet on the effective value of the Planck constant. They found that this dependence significantly differs from the prediction of the theory developed earlier by Wilkinson [12, 13] and argue that the observed difference is the result of chaos.

The behavior of the splitting of quasidegenerate doublets has also been the subject of the recent paper by Bohigas *et al.* [14]. Using the autonomous system of two coupled quartic oscillators they demonstrated that tunneling is strongly affected by classical integrability of the Hamiltonian system. Beyond the quasi-integrable regime the splitting becomes extremely sensitive to variations of the external parameter. To quantify the observed phenomenon they considered a three-level model which describes the interaction of the chaotic eigenstate with the quasidegenerate doublet. They conclude that "the major consequence of chaos is enhanced tunneling between islands by allowing transport across regions in phase space." In a previous paper [15] we pointed out that the above scenario is valid only for sufficiently small coupling between the regular doublet and the chaotic state, a condition which may be satisfied far enough from the center of the avoided crossing. In the neighborhood close to the center of the crossing quantum dynamics is very different. This difference is associated with the interchange of the structure of the interacting states, a generic quantum property of a two-level system.

The purpose here is to present a thorough discussion of the avoided level crossing involving a regular doublet state localized on symmetric KAM islands and a third chaotic state. We refer to this type of avoided crossing as *chaos-induced avoided level crossing* or *chaotic avoided level crossing* [15] and examine its implications on the

phase space tunneling. Herein we analyze the part of the Floquet spectrum different from that used previously [15]. This choice is somewhat more suitable for the discussion of phase space tunneling than that used previously.

The paper is organized as follows. In Sec. II we introduce our model system — the harmonically driven pendulum — and give a brief review of the Floquet formalism. We describe the algorithm used to generate the Husimi representation of quasienergy states and wave functions. Section III is devoted to the analysis of the chaotic avoided level crossing phenomenon. We begin with a discussion of the general characteristics of the quasienergy states of the driven pendulum. Then using the Husimi representation of quantum mechanics we elucidate the relation between the structure of the Floquet states involved in the avoided crossing and the Poincaré surface of section of the driven pendulum. In Sec. IV we study the quantum dynamics of wave packets originally localized on the symmetric KAM islands. Such packets were formed by taking symmetric or antisymmetric combinations of the doublet states far away from the crossing. We show that as a consequence of the avoided level crossing phenomenon the initial simple two-level dynamics is replaced by the much more complicated dynamics involving three quasienergy states. This three-level dynamics can give rise to a variety of different quantum motions. In particular, in the center of the avoided crossing, i.e., the point where the energy differences between states are equal, the rate of the tunneling may be significantly enhanced. Away from the center the quantum dynamics is usually quasiperiodic, but in some cases it is intricate and very different from the simple dynamics usually associated with tunneling. In Sec. V we draw some conclusions. The procedure used to numerically integrate the time dependent Schrödinger equation is discussed in the Appendix.

II. DRIVEN PENDULUM MODEL

As our model system we choose the driven pendulum

$$H = H_0 - \mu\gamma q\cos(\Omega t), \tag{1}$$

where the unperturbed Hamiltonian H_0 reads

$$H_0 = \frac{p^2}{2\mu} + \mu(1+\cos q), \tag{2}$$

γ is the peak amplitude of the driving force, and Ω is its frequency. Performing the trivial scaling of the angular momentum by the parameter μ, $p' = p/\mu$, the Hamilton's equations of motion generated by (1) may be expressed in a form independent of μ. In the quantum domain this scaling parameter plays a much more significant role. It may be interpreted as the inverse of the "effective" Planck's constant since the limit $\mu \to \infty$ is equivalent to the semiclassical limit. The angle varies between 0 and 2π contrary to the conventional range $[-\pi, \pi]$. This modification was introduced to facilitate quantum calculations, but otherwise does not affect the classical or quantum properties of the model. In all classical and quantum simulations discussed in this paper $\Omega = 2$ and $\mu = 5$. The unperturbed Hamiltonian H_0, i.e., the pendulum, has become the paradigm for nonlinear dynamics [16]. The driven model has also been extensively studied in the context of particle beam stability in large accelerators [17,18]. Using the Wigner and Husimi representation of quantum mechanics Lee and Feit [19] have recently investigated quantum manifestations of chaos in systems described by the driven damped pendulum.

The Hamiltonian (1) remains invariant under the following set of the symmetry operations:

$$q \to -q,\ t \to t + \pi/\Omega. \tag{3}$$

The dynamical symmetry (3) is identical to that of the driven double well potential and we expect that the generic properties of the driven pendulum hold true for a large class of bounded Hamiltonian systems exhibiting this kind of symmetry. In order to optimize the quantum mechanical calculations we use a gauge invariant form of the Hamiltonian (1) generated by the following transformations:

$$A'(t) = A(t) + \frac{\partial}{\partial q}\chi(q,t) = -\frac{\mu\gamma}{\Omega}\sin(\Omega t), \tag{4}$$

$$V'(q) = V(q,t) - \frac{\partial}{\partial t}\chi(q,t) = \mu(1+\cos q), \tag{5}$$

where $\chi(q,t) = -\mu\gamma q\sin(\Omega t)/\Omega$, the vector potential $A(t)$ is identically equal to zero, and $V(q,t) = \mu(1+\cos q) - \mu\gamma q\cos(\Omega t)$. Then the gauge invariant Hamiltonian H_χ is given by

$$H_\chi = \frac{1}{2\mu}[p - A'(t)]^2 + V'(q) \tag{6}$$

and the solution of the time-dependent Schrödinger equation corresponding to (6) may be formally written as

$$|\psi(t)\rangle = \exp_T[-i\int_0^t H_\chi(t')dt']|\psi(0)\rangle. \tag{7}$$

In the above equation and the rest of this paper Planck's constant was set to unity. In the most straightforward approach the wave function (7) is expanded in the basis of the eigenfunctions of the angular momentum operator $\hat{p}$:

$$|\psi(t)\rangle = \sum_{n=-n_{\max}}^{n_{\max}} c_n(t)|\phi_n\rangle. \tag{8}$$

The detailed discussion of the numerical procedure employed to solve the time-dependent Schrödinger equation is presented in the Appendix.

The periodicity of the Hamiltonian (1) enables us to describe quantum evolution in terms of the Floquet theory. An extensive review of this approach is given by Chu [20]. Within the framework of the Floquet formalism the time evolution is determined via successive application of a one-cycle unitary propagator $\hat{C}$, which maps the wave function at time t into the wave function at time $t+T$. The eigenvalue problem for the propagator $\hat{C}$ may be written as

$$\hat{C}|\lambda_n\rangle = \exp(-iE_n)|\lambda_n\rangle, \tag{9}$$

where the E_n are called quasienergies and for a bounded system are real numbers. The corresponding eigenfunctions $|\lambda_n\rangle$ are referred to as quasienergy states or Floquet states. It may be shown that they are the eigenvectors of the Hermitian operator $\hat{H} - i\hbar\partial/\partial t$ and consequently form a complete orthonormal basis. In the case of the driven pendulum the Floquet states may be classified into states of even and odd parity with respect to the generalized parity transformation (3). To obtain the matrix representation of $\hat{C}$ in the angular momentum eigenbasis notice that

$$\langle\phi_j|\psi(T)\rangle = \sum_k \langle\phi_j|\hat{C}|\phi_k\rangle\langle\phi_k|\psi(0)\rangle \tag{10}$$

and if we choose the initial state such that

$$\langle\phi_k|\psi(0)\rangle = \delta_{k,j'}, \tag{11}$$

then

$$\langle\phi_j|\psi(T)\rangle = \langle\phi_j|\hat{C}|\phi_{j'}\rangle. \tag{12}$$

Thus the j' column of the matrix representation of $\hat{C}$ may be calculated using the initial conditions (11) and integrating the time-dependent Schrödinger equation over one period of the perturbation. We can then numerically solve the eigenvalue problem (9). For times $t = kT$, $k = 1, 2, \ldots$ the wave function may be written as

$$|\psi(kT)\rangle = \sum_n \exp(-iE_n k)|\lambda_n\rangle\langle\lambda_n|\psi(0)\rangle. \tag{13}$$

It is apparent from (13) that only the Floquet states overlapping the initial wave function contribute to its subsequent time evolution. These states are frequently referred to as the Floquet spectrum of the wave function.

Properties of classical dynamics are conveniently studied in a phase space representation. The uncertainty principle precludes the direct transfer of this concept and that of distribution functions to quantum mechanics. Nonetheless the so-called quasiprobability distribution functions [21] have proved to be extremely useful in studying the correspondence between classical and quantum mechanics. They provide also deep insight into the morphology of quasienergy states (their relation to the structure of the corresponding classical phase space). In this paper we adopt the Husimi representation [22, 23], which for a system in state $|\psi\rangle$ may be defined as

$$\rho(q,p) = \frac{1}{2\pi}|\langle\psi|\Phi_{pq}\rangle|^2, \tag{14}$$

where

$$\Phi_{pq}(q') = \frac{1}{(2\pi\sigma^2)^{1/4}} \exp\left[\frac{-(q'-q)^2}{4\sigma^2} + ipq'\right] \tag{15}$$

is the coherent state and σ is a coarse graining parameter. For all Husimi distributions displayed in this paper $\sigma^2 = 0.07$. This choice assured faithful phase space representation of all presented quasienergy states and wave functions. The problem of selecting a value of coarse graining parameter in the Husimi representation is discussed in more detail in Refs. [24, 25]. Using the expansion (8) we may rewrite (14) as

$$\rho(q,p,t) = \frac{1}{2\pi}\left|\sum_n c_n^*(t)\langle\phi_n|\Phi_{pq}\rangle\right|^2. \tag{16}$$

Thus the evaluation of the Husimi distribution essentially amounts to the calculation of the Fourier spectrum of the coherent state. We do not write down the lengthy analytic expression for the Fourier coefficients since they may be readily obtained with the help of many symbolic algebra packages (e.g., Mathematica). The fast Fourier transform algorithm provides an alternative numerical and very efficient method of determination of the Fourier coefficients.

III. CHAOTIC AVOIDED LEVEL CROSSING

The Floquet spectra of one-dimensional driven systems are usually intricate functions of the amplitude of the perturbation. For small amplitudes of the driving force it is possible to establish a connection between individual quasienergy states and the stationary eigenfunctions from which they evolve. The Floquet states undergo a series of apparent level crossings and avoided level crossings which renders this analysis increasingly formidable as the perturbation strength increases. In Fig. 1(a) we present a portion of the Floquet spectrum of the driven pendulum which was obtained via numerical diagonalization of the one-cycle propagator $\hat{C}$. While some of the quasienergy states remain weakly affected by the perturbation and form characteristic horizontal bands others are strongly influenced as indicated by the rapid change of the corresponding quasienergies (note that the entire spectrum is confined to the interval$[-\pi, \pi]$). What appears as two of the quickly evolving states "cross" in the central part of the Fig. 1(a) bounded by the rectangle. The enlargement of this region given in Fig. 1(b) reveals, however, the characteristic double cone structure of the avoided level crossing [26, 27] which originates as a result of interaction between a member of the nearly degenerate doublet A and the quasienergy state B, both having the same symmetry. The other member of the doublet, labeled in Fig. 1(b) by C, has a dynamical symmetry opposite to those of states A and B. If one approximates the observed crossing with the help of a three-level model, for example, choosing as a basis Floquet states far enough from the center of the crossing, then the selection rules reduce the problem to the interaction between states A and B. The other state does not play any role in this process. To elucidate the nature of the avoided level crossing displayed in Fig. 1(b) let us examine the connection between the classical phase space portrait and the structure of the Floquet states A, B, and C. We precede this analysis with a brief overview of the general properties of the quasienergy states of the driven pendulum.

Figure 2 shows the Poincaré surface of section calculated for $\gamma = 0.88$. One can see that chaotic trajectories

which originally developed only in the region of the separatrix now occupy a much larger part of the phase space. However, the phase space portrait still retains the essential features of the dynamics of the unperturbed pendulum. There are noticeably deformed tori corresponding to oscillations around the elliptic fixed point $(0,0)$. The KAM tori associated with rotations may be found for $|p| > 2.1$. With the growing absolute value of the angular momentum, tori become less distorted and closely resemble those of unperturbed rotations. The novel phase space structures are the nonlinear resonances. In Fig. 2 we present only these resonances which are relevant for further discussion; they are immersed in the stochastic sea.

Now the question arises to what extent the structure of the classical phase space influences quasienergy states. To address this problem in Fig. 3 we sorted the Floquet states (computed at $\gamma = 0.88$) with respect to their expectation value of the angular momentum $\hat{p}$. One can see that the states roughly fall into either of two categories. Within one category the average momentum grows linearly with state number as in the case of the angular momentum operator. Thus we expect that these states represent clockwise and counterclockwise rotations. The other group comprises states with the expectation value of the angular momentum close to zero. In this case the identification of the nature of these states is more complicated. The criterion based solely on the average value of the momentum cannot, for example, distinguish between Floquet states associated with oscillations around the elliptic point $(0,0)$ and "chaotic states" strongly influenced by the stochastic sea. Although Fig. 3 provides useful intuition about the character of the quasienergy states of the driven pendulum, much more information may be derived from a comparison of their phase space representations and the classical phase space.

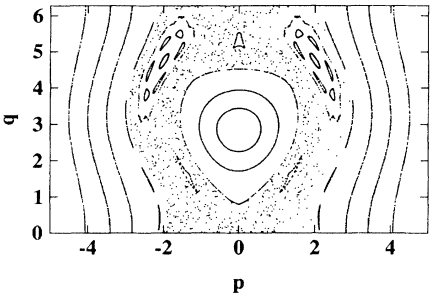

FIG. 2. Poincaré surface of section for the driven pendulum with $\Omega = 2, \mu = 5$, and $\gamma = 0.88$. Momentum was scaled by the parameter μ.

In Fig. 4 we present the Husimi distribution of quasienergies A, B, and C calculated for the same value of the amplitude γ as that used in Fig. 2. In accompanying contour plots six basic contour lines uniformly spaced between zero and maximum value were used. Each contour plot was superimposed with the KAM tori taken from Fig. 2 (heavy dots). The Husimi distributions of states A and C shown in Figs. 4(a) and 4(b), respectively, are very similar to each other as one would expect from the members of the quasidegenerate doublet. Both distributions are centered on the prominent symmetric nonlinear resonances immersed in the chaotic sea. Note that the very well localized distributions are not entirely confined by the outermost KAM tori which delineate the islands and clearly leak into the stochastic part of the phase space. The intricate, self-similar structure of smaller resonances within the islands is not manifested

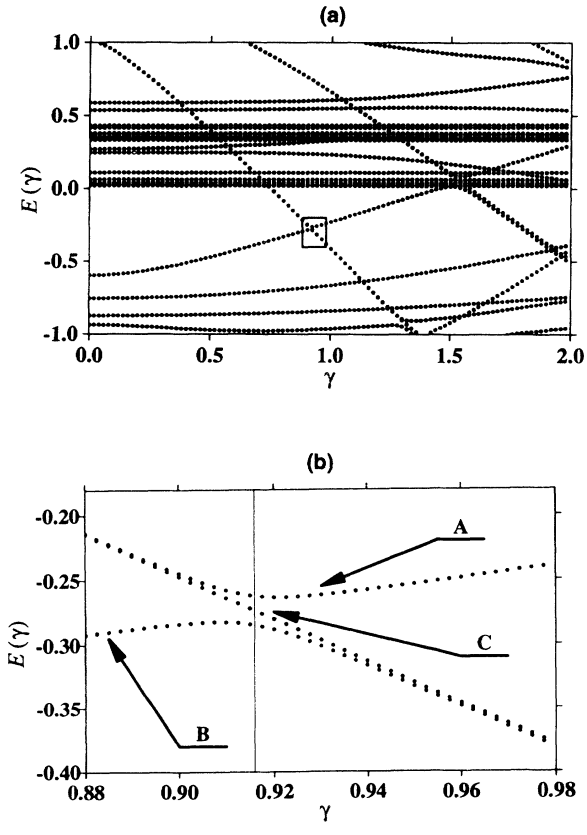

FIG. 1. (a) Floquet spectrum of the driven pendulum as a function of the amplitude of the driving force ($\Omega = 2$ and $\mu = 5$). (b) The small rectangular part of (a) is magnified to show the avoided crossing between the quasienergy state B and a member of nearly degenerate doublet A. The vertical grid line indicates the center of the crossing.

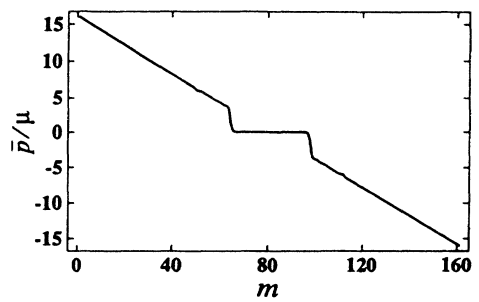

FIG. 3. The expectation value of momentum for the Floquet states determined for $\gamma = 0.88$. This picture elucidates the influence of structure of the classical phase space on the morphology of quasienergy states.

by the distributions of quasienergy states A and C. However, the size of these resonances is much smaller than the effective Planck constant. Despite the similarity of the Husimi representations of states A and C, the analysis of Fig. 4(a) reveals the existence of a hardly noticeable narrow isthmus which joins the humps of the distribution. In the corresponding contour plot this isthmus was resolved using the additional contour line. This distinctive feature of the distribution of the Floquet state A is absent in Fig. 4(b), which shows the distribution of the state C. The physical interpretation of this difference shall be given subsequently. The nature of the state B [cf. Fig. 4(c)] is utterly different from that of the doublet states A and C. It is spread in the chaotic part of the phase space and only slightly overlaps the central regular region of the classical phase space. We can see that its quantum distribution embodies three small resonances around the fixed point of the periodic orbit [the coordinates of the upper fixed point are $(0, 5.312)$]. To better understand the structure of this state in Fig. 5 we display its Husimi representation obtained for a much weaker driving force $\gamma = 0.25$. For this value of the perturbation the resonances around the fixed points are much larger and it is apparent that they underline the shape of the distribution. With the growing amplitude of the driving force these resonances shrink, but the quasienergy state retains

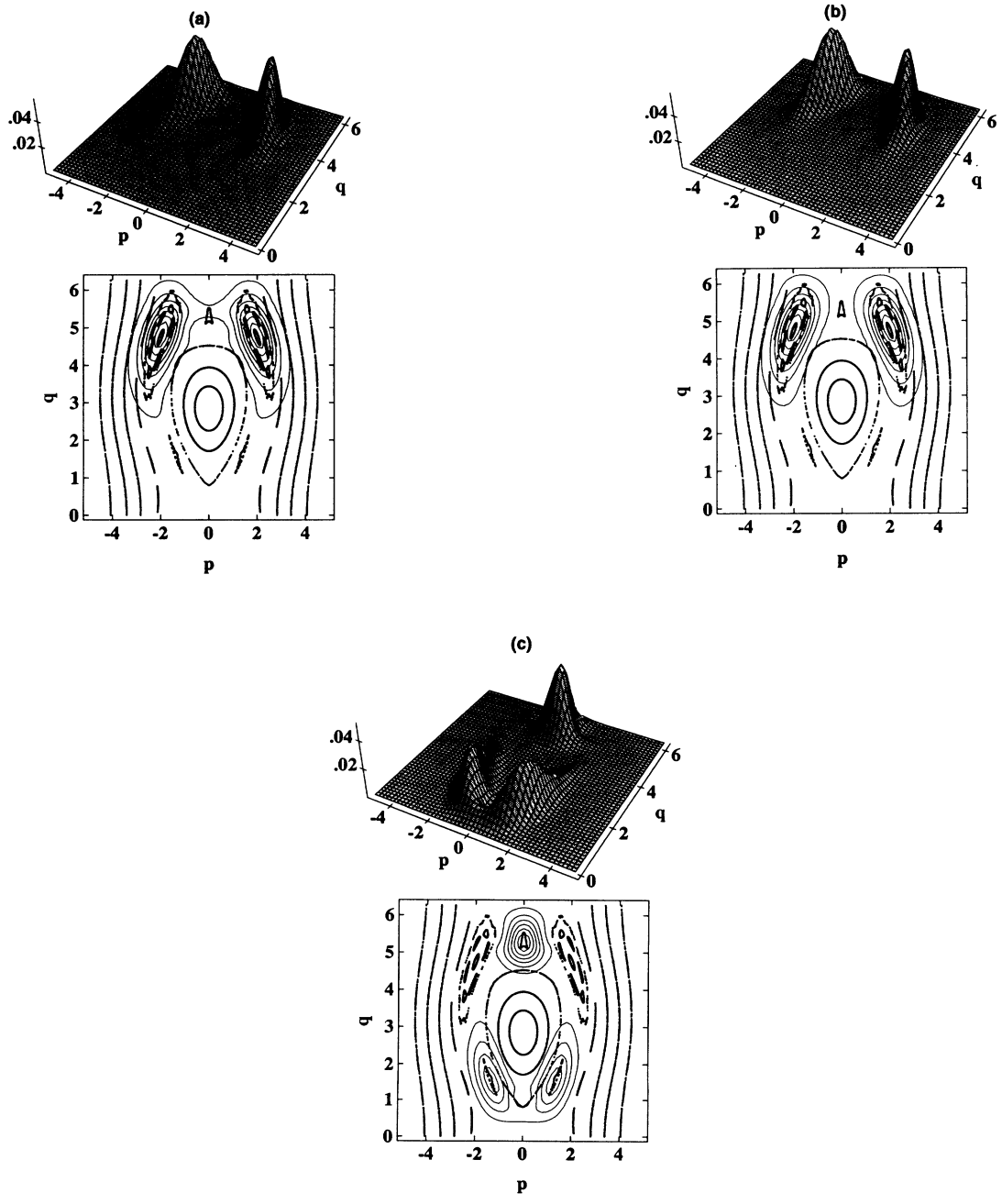

FIG. 4. Husimi representation of the Floquet states shown in Fig. 1(b). Momentum was scaled by the parameter μ. The model parameters are the same as in Fig. 2. (a) corresponds to quasienergy state A, (b) to state C, and (c) to B.

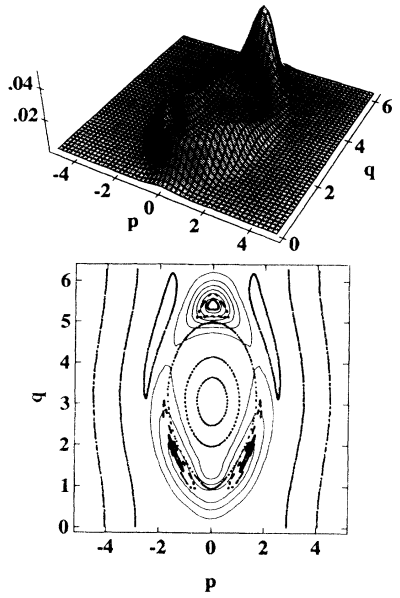

FIG. 5. Husimi representation of the Floquet state B for the small value of the amplitude of the driving force $\gamma = 0.25$. Momentum was scaled by the parameter μ. Notice the much larger size of the nonlinear resonance which underlines the structure of this state.

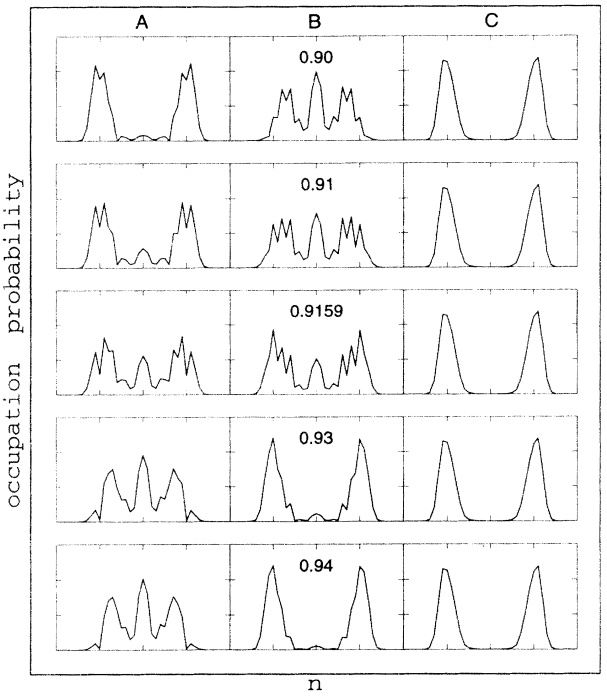

FIG. 6. Expansion of Floquet states A, B, and C in the basis of the eigenfunctions of angular momentum operator plotted for five values of the amplitude γ chosen from the interval $[0.90, 0.94]$. Note that this interval comprises the main part of the avoided crossing shown in Fig. 1(b). In all graphs quantum number n varies between -20 and 20. The range of occupation probability is $[0, 0.15]$.

its three peak structure, which begins to emerge in Fig. 5 and is quite well developed in Fig. 4(c).

We have already mentioned that the repulsion between states A and B may be well approximated by a simple two-level model. Far enough from the center of the avoided crossing the Husimi representation of the doublet states A and C are essentially indistinguishable. The contamination of the Husimi distribution of state A by a chaotic component in Fig. 4(a) is a precursor of the complete exchange of the structure between initially regular (localized) state A and originally delocalized state B. This purely quantum mechanical process, characteristic for a two level system, is elucidated in Fig. 6. In this figure the expansion of all three states in the basis of eigenfunction of the angular momentum operator $|\phi_n\rangle$ are plotted for five values of the amplitude γ chosen from the interval $[0.90, 0.94]$. The inspection of Fig. 1(b) shows that this interval comprises the main part of the avoided level crossing. In all the graphs in Fig. 6 the quantum number n varies between -20 and 20, the range of occupation probability is $[0, 0.15]$. From the first panel in Fig. 6, which corresponds to the amplitude $\gamma = 0.90$, it is apparent that the repulsion has already appreciably influenced the structure of both states A and B. The former one is still similar to its doublet counterpart C, but now populates the basis states that span the initially chaotic state B.

We can see in Fig. 6 that with the growing perturbation the mixing of states A and B become more strongly pronounced so that at $\gamma = 0.9159$ (approximate center of the crossing) they look very much alike. This mixing is further elucidated in Fig. 7, which shows the Husimi representation of the states A and B at this particular value of the amplitude. It is apparent that both quantum distributions, while bearing some resemblance to the distribution of state C, are delocalized in the chaotic part of the phase space. At this point the linear combinations of states A and C no longer yield a wave packet localized in the symmetric parts of the phase space, the property which is the hallmark of phase space tunneling. We do not present the Husimi distribution of the state C corresponding to $\gamma = 0.9159$ since, as expected from the symmetry analysis, this state is not affected by the crossing and changes insignificantly in the range of perturbation shown in Fig. 1(b).

If the amplitude of the driving force is further increased the "rotation" of quasienergy states A and B proceeds and at $\gamma = 0.94$ they almost completely exchange their structure (cf. the first and the last panel in Fig. 6). The initially chaotic state becomes fairly regular and the initially regular state becomes chaotic. From Fig. 1(b) we can infer that with the growing perturbation the splitting between states B and C steadily decreases. Thus subsequent phase space tunneling is determined by the newly formed doublet made up of states B and C.

Now let us assess the role of classical chaos in the phenomenon discussed above. The avoided level crossing does not take place until the chaotic Floquet state significantly populates levels which span the nearly degenerate doublet. The KAM tori have been shown to persist in the quantum phase space as dynamical barriers which inhibit wave functions from exploring classically forbidden

regions of phase space [28, 29]. For a sufficiently small value of Planck's constant the properties of the classical phase space are clearly reflected in the structure of the Floquet states [30–35]. The kind of avoided level crossing displayed in Fig. 1(b) may occur for sufficiently strong interaction between the chaotic state and the member of the quasidegenerate doublet. This kind of interaction takes place only if the phase space representation of the doublet states are not entirely enclosed by the KAM tori and consequently appreciable overlap the distribution of the third state associated with the chaotic sea. We have not been able to observe any detectable change in the level splitting when the doublet crosses the path of several rotational states shown in Fig. 1(a) (they form a characteristic horizontal band). The Husimi distribution of the latter states are entirely isolated from those of the doublet. Thus we can see that chaos influences all levels involved in the avoided level crossing displayed in Fig. 1(b) and why we used the term *chaos-induced avoided level crossings or chaotic avoided level crossings* to describe its nature [15]. We emphasize that the avoided crossing between a tunneling doublet and a regular state [e.g., one associated with the large island around the elliptic fixed point $(0,0)$] is quite conceivable. However, our analysis of the Floquet spectrum of the driven pendulum shows that this type of crossing is significantly less prevalent than the one involving a third state associated with the stochastic layer.

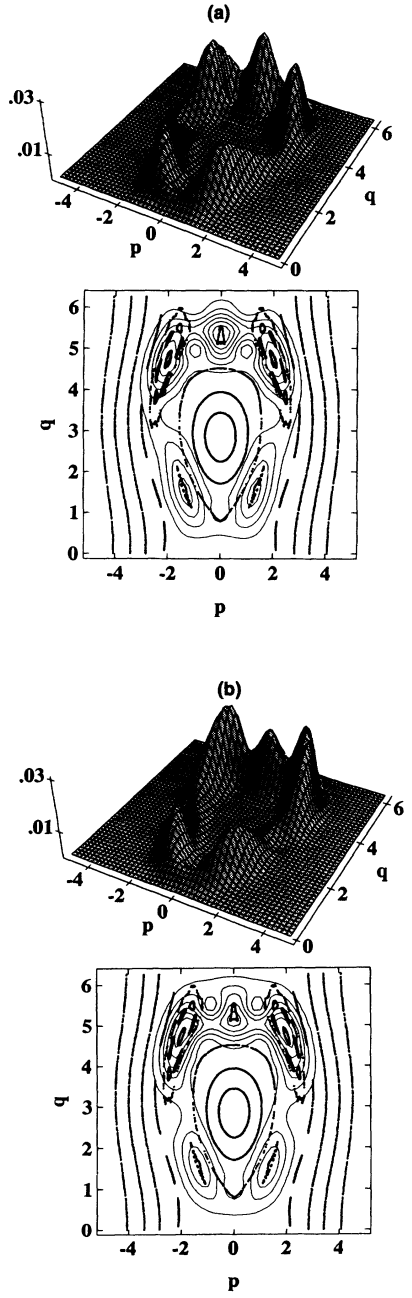

FIG. 7. Husimi representation of the Floquet states shown in Fig. 1(b) at the center of the avoided crossing. Momentum was scaled by the parameter μ. (a) corresponds to quasienergy state A, (b) to B.

IV. THREE-LEVEL DYNAMICAL TUNNELING

We have pointed out in Sec. III that the tunneling produced by the quasidegenerate doublet originally made up of states A and C is destroyed as the result of the avoided level crossing. With the growing amplitude of the driving force state A gradually loses its initial character so that at the center of the crossing the combination of states A and C no longer yields localized wave packets. Thus the increased splitting of the doublet does not imply enhanced dynamical tunneling.

In this section we investigate the influence of the chaotic avoided crossing on the quantum dynamics of a wave packet centered on one of the symmetric KAM islands shown in Fig. 2. Such a wave packet may be formed by taking the symmetric or antisymmetric superposition of the doublet states when the parameter γ is far from the value at the center of the crossing. In Fig. 8 we present the Husimi distribution of the symmetric combination of states A and C at $\gamma = 0.90$. We examine the dynamics of this wave packet for different values of the amplitude of the driving force and describe the time evolution of the wave function with the help of the *quantum survival probability* or *autocorrelation function*:

$$S(t) = |\langle\psi(0)|\psi(t)\rangle|^2. \tag{17}$$

At $\gamma = 0.90$ the wave packet is spanned only by states A

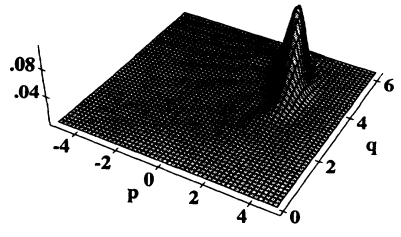

FIG. 8. Husimi representation of the symmetric combination of the quasienergy states A and C calculated for $\gamma = 0.90$.

and C; consequently its dynamical behavior is quite simple. In fact, using (13) and (17) the survival probability at the integer multiples of the period may be written as

$$S(kT) = \frac{1}{2} + \frac{1}{2}\cos[(E_1 - E_3)k], \tag{18}$$

where E_1 and E_3 are the quasienergies of states A and C, respectively. Thus the wave function harmonically oscillates between the symmetric KAM islands. In Fig. 9 we show the time development of the survival probability (solid thin line) at $\gamma = 0.90$. The wave function was generated by the repetitive application of the one-cycle propagator $\hat{C}$. The full circles in this figure are the values of the autocorrelation function obtained with the help of formula (18). If, on the other hand, we use the same wave packet as the initial condition but increase the strength of the driving, then the dynamics gets more involved.

Due to repulsion between the member of the doublet A and the chaotic state B the wave packet becomes the linear superposition of all three quasienergy states A, B, and C. In Fig. 10 we can see that with growing perturbation the occupation probability flows from state A to B. This process takes place since the avoided level crossing involves the exchange of the structure of these states. The initially regular state A turns into the chaotic state B and vice versa. As we mentioned earlier, the state C is not affected by the avoided crossing and its occupation probability remains constant. The selected values of the amplitude γ in Fig. 10 are the same as those used in Fig. 6. Again using Eqs. (13) and (17) we derive the survival probability for the three-level dynamics:

$$S(kT) = \sum_{i=1}^{3} d_i^2 + 2\sum_{\substack{i,j=1 \\ i<j}}^{3} d_i d_j \cos[(E_i - E_j)k], \tag{19}$$

where $d_i = |\langle\psi(0)|\lambda_i\rangle|^2$; $|\lambda_1\rangle$, and $|\lambda_2\rangle$, and $|\lambda_3\rangle$ denote the Floquet states A, B, and C, respectively.

It is apparent from the above equation that in general there are three frequency differences $(E_i - E_j)$ involved in the packet's dynamics. They may give rise to a variety of different motions as exemplified in Fig 11. Figure 11(a) corresponds to the amplitude $\gamma = 0.915$. In this case the evolution of the survival probability appears to be quasiperiodic. The vertical grid lines are used to indicate

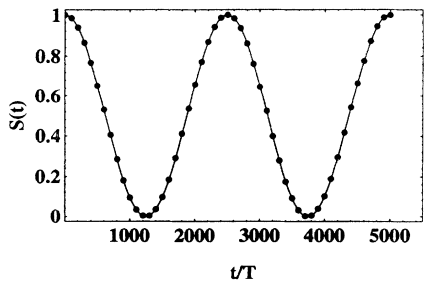

FIG. 9. Time evolution of the survival probability (solid line) for the wave packet from Fig. 8, $\gamma = 0.90$. Dots are the values calculated from Eq. (22). Dots are the values calculated from Eq. (22).

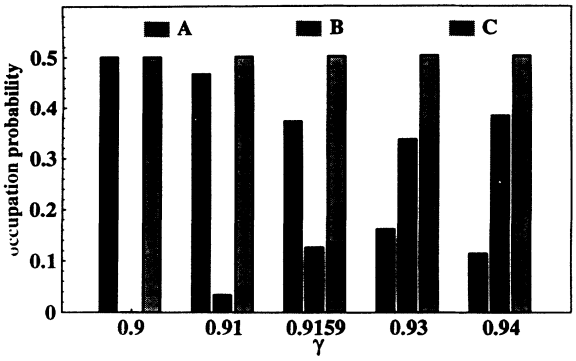

FIG. 10. Expansion of the wave packet from Fig. 8 in the Floquet basis determined for different values of the amplitude γ.

the quasiperiod. Within the quasiperiod the wave packet tunnels from one island to the other in a time shorter than that for the conditions in Fig. 9. However, one can see that the intermediate collapses and revivals are usually not complete. The situation at the center of the crossing [marked in Fig. 1(b) by the vertical grid line] is quite different.

At the center point there are only two different frequency differences since $E_1 - E_2 = 2(E_1 - E_3) = 2(E_3 - E_2)$. Furthermore, if we notice that $\sum_i d_i = 1$ and $d_3 = 0.5$, then Eq. (19) may be rewritten as

$$S(kT) = \frac{1}{2}\{1 + \cos[(E_1 - E_3)k]\} - 4d_1 d_2 \sin^2[(E_1 - E_3)k]. \tag{20}$$

The first term in the above equation determines the functional form of the survival probability. The other term introduces only minor modifications. Thus at the center of the crossing the wave packet periodically oscillates between the KAM islands. These oscillations are shown in Fig. 11(b). The filled circles represent the values of the autocorrelation function calculated from formula (20). Note that the tunneling rate is determined only by the splitting $E_1 - E_3$, but not by the structure of the Floquet states A and B, which enter into (20) via the coefficients d_1 and d_2. So far we have tacitly assumed that the survival probability approaches zero whenever the wave function reassembles itself after tunneling on the symmetric counterpart of the KAM island from which the packet was launched. This process is shown in Fig. 12, where the Husimi representation of the wave packet at $t = 140T$ and $t = 281T$ are given. These times approximately correspond to a quarter and to a half of the period of the oscillations. It is quite surprising how clearly the wave function at $t = 140T$ resembles the Floquet states A and B from Fig. 7. Away from the center of the avoided crossing the periodicity of the quantum dynamics is lost. This is demonstrated by the rapid change of the pattern of the oscillations for $\gamma = 0.93$ in Fig. 11(c). For even stronger perturbation, such as $\gamma = 0.95$ in Fig. 11(d), the dynamics is dominated by the newly formed doublet made up of states B and C. We can see that the low frequency oscillation, very similar to that in Fig. 9, is

superimposed with much lower amplitude high frequency oscillations. This type of dynamics appears in the limit of the small coupling between the chaotic state and one of the doublet states [14], the condition which is satisfied far enough from the center of the avoided crossing. Unlike the strong coupling case shown in Fig. 12, the wave packet tunnels between the KAM islands without fully appearing in the stochastic sea. Figure 13 shows the Husimi representation of the wave function in the numerical experiment from Fig. 11(d) at $t = 544T$. This time corresponds to a local minimum of the fast oscillations of the survival probability. One can see that only a small portion of the wave packet, which broke off from the hump localized on the right torus, shows up in the chaotic sea. During the following half of the period of the rapid oscillations this small piece moves to the symmetric (left) torus so that at the local maximum of the survival probability the penetration of the stochastic layer is hardly noticeable. The complete tunneling of the wave packet is accomplished via the incremental transport of the small pieces across the stochastic sea. Note that the excellent agreement of the survival probability in Fig. 11 with the values obtained from Eqs. (19) and (20) arises from the validity of the three-level approximation used to describe the avoided level crossing phenomenon.

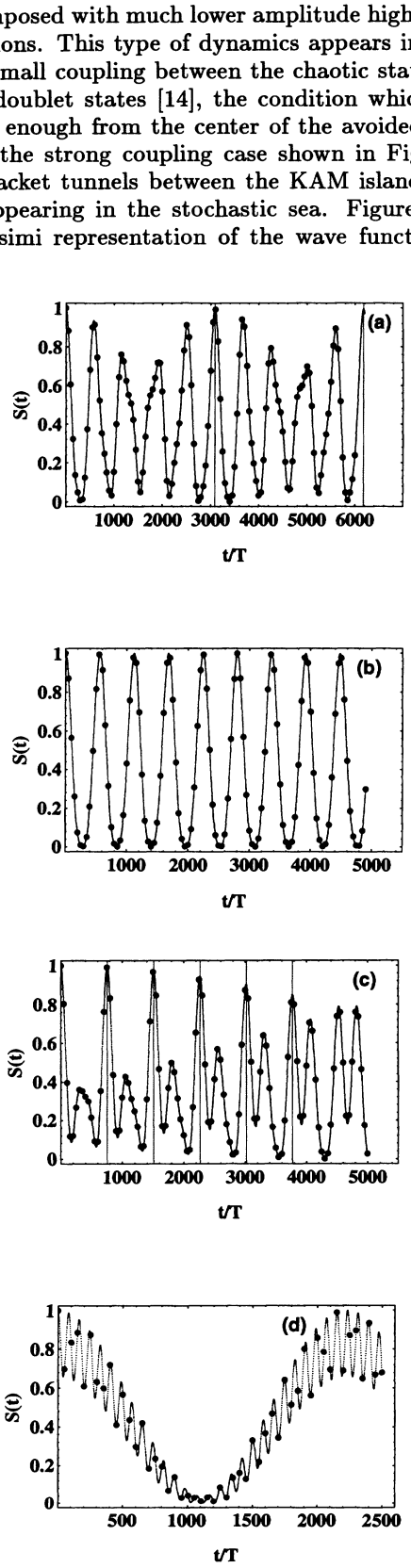

FIG. 11. Time evolution of the survival probability for the wave packet from Fig. 8 for different values of the amplitude of the driving force: (a) $\gamma = 0.915$, (b) $\gamma = 0.9159$, (c) $\gamma = 0.93$ and (d) $\gamma = 0.95$.

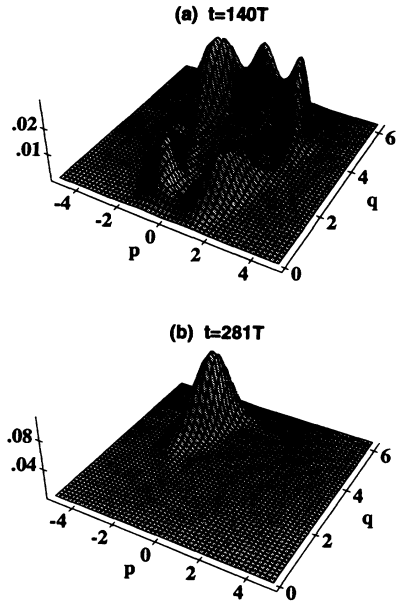

FIG. 12. Husimi representation of the wave packet in the numerical experiment from Fig. 11(b) calculated at (a) $t = 140T$ and (b) $t = 281T$.

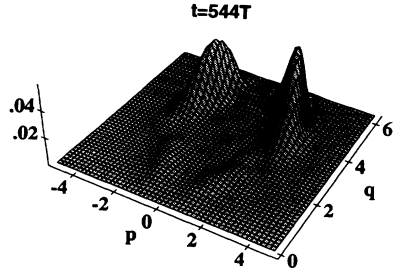

FIG. 13. Husimi representation of the wave packet in the numerical experiment from Fig. 11(d) calculated at $t = 544T$.

V. CONCLUSIONS

In this paper we investigated the interplay of chaos and dynamical tunneling in the driven pendulum. We analyzed the avoided level crossing between the Floquet state associated with the chaotic part of the classical phase space and the member of the quasidegenerate doublet whose quantum distribution is localized on the symmetric KAM islands. We dubbed this phenomenon *chaos-induced avoided level crossing* or *chaotic avoided crossing* to emphasize the fact that all involved quasienergy states are influenced by the presence of the chaotic sea. We pointed out that the exchange of the structure of the interacting states, the process inherent to two-level model, leads to the destruction of tunneling produced by the members of the original doublet and gives rise to the formation of a new doublet. We also studied the implications of this effect on the quantum dynamics of a wave packet centered on one of the symmetric KAM islands. To clarify the discussion we generated such a wave packet by taking the superposition of the doublet states far away from the center of the crossing. Employing the quantum survival probability, we showed that within the parameter region comprising the avoided crossing the initially trivial two-level dynamics is superseded by a more complicated dynamics involving three quasienergy states. In the latter case, the dynamical behavior may vary from quasiperiodic motion to quite intricate motion distinctly different from the simple dynamics usually associated with tunneling. However, we found that at the center of the avoided crossing the tunneling is always enhanced and recovers the perfectly periodic character. We derived the simple formula (20), which indicates that at the center point the tunneling rate is determined exclusively by the minimal width of the crossing, but does not depend upon the structure of the quasienergy states.

The recent surge of scientific activity concerning phase space tunneling is stimulated by the emerging possibilities of the experimental verification of such theoretical concepts. For example, Leo *et al.* [36] observed the oscillations of the wave packet created in a GaAs/AlGaAs double quantum well structure (DQWS) by ultrashort pulse excitation. By varying the applied force they observed the suppression of the tunneling at the exact crossing of the hybridized excited states. The theoretical analysis of this affect was given by Grossman *et al.* [6–9]. We already pointed out that the dynamical symmetry of the driven pendulum is identical to that of the driven double well potential whose experimental realizations are feasible in various fields, e.g., ammonia molecule, DQWS, or a rf driven superconducting quantum interference device. The question arises whether chaos-induced avoided level crossing may be observed experimentally. The important property which might facilitate an actual experiment is the discussed enhancement of the three level tunneling at the center of the crossing. Moreover, we have found that this type of tunneling is particularly robust against any symmetry breaking perturbation, which distinguishes it from ordinary tunneling involving two states. The further discussion of this issue will be presented elsewhere [37].

Some thirty years ago Mark Kac asked the following famous question: "Can we hear the shape of a drum?" [38]. Several years later Davis and Heller, in their pioneering investigation of the dynamical tunneling [1], pointed out in the same spirit that "eigenvalues are not the whole story of bound state quantum mechanics." We are convinced that this remark reflects the nature of the phenomenon discussed in this paper.

ACKNOWLEDGMENTS

We gratefully acknowledge discussions with Dr. F. Izrailev and Dr. S. Tomsovic. This work was supported by the Texas National Research Laboratory Commission (Project No. RGFY93-203). The authors thank the National Science Foundation for support of the numerical calculations performed on the Cray C90 supercomputer at the Pittsburgh Supercomputing Center (Grant No. PHY920023P).

APPENDIX

In order to find the numerical solution to the time-dependent Schrödinger equation (7) we employ the expansion (8) and approximate the time dependence of the vector potential (6) by [39]

$$\hat{A}'(t) = -\frac{\Delta t \mu\gamma \sin(\Omega t)}{\Omega} \sum_k \delta(t - k\Delta t) \tag{A1}$$

with $\Delta t = 2\pi/(\Omega L)$, where L is the number of integration steps taken per period of the driving force. Then the integration in (7) may be carried out analytically and the vector of the expansion $\mathbf{c}(t_k + \Delta t)$ coefficients at time $t_k + \Delta t$ ($t_k = k\Delta t$) may be obtained by the successive multiplication of vector $\mathbf{c}(t_k)$ at time t_k by unitary matrices:

$$\mathbf{c}(t_k + \Delta t) = UQVQ^{-1}\mathbf{c}(t_k). \tag{A2}$$

U and V are both diagonal matrices with

$$U_{n,n} = \exp\left\{-i\Delta t\left[\frac{n^2}{2\mu} + \frac{n\gamma \sin(\Omega t_k)}{\Omega}\right]\right\} \tag{A3}$$

and

$$V_{n,n} = \exp(-i\Delta t \nu_n). \tag{A4}$$

ν_n are the eigenvalues of the matrix representation N of the operator $\mu\cos(\hat{q})$ in the basis of the angular momentum operator eigenfunctions. Q is a unitary matrix that transforms N into diagonal form ($N = QVQ^{-1}$). The advantage of the gauge transformation is now apparent. Both the kinetic energy operator and the time-dependent perturbation are diagonal in the angular momentum eigenbasis, which significantly enhances the computational efficiency. Moreover, the symmetric matrix N has an extremely simple structure: $N_{n,m} = (\delta_{m,n+1} + \delta_{m,n-1})(\mu/2)$, and consequently may be easily diagonalized. In (A2) we have neglected the contribution originating from $\hat{A}'^2$ term and constant μ term since they

only yield global phase factors. Note that the genuine solution of the Schrödinger equation corresponding to the Hamiltonian (1) is given by $\exp[i\chi(q,t)]|\psi(t)\rangle$. However, in this work we calculated the wave functions only at the integer multiple of the period T. In this case the wave functions in both gauge invariant representations coincide due to the periodicity of $\chi(q,t)$. We have found this integration scheme to be very reliable. It preserves the norm of the wave function with high accuracy, which was particularly important in our studies of the long time quantum dynamics discussed in Sec. IV. In quantum calculations $L = 300$, although acceptable accuracy may be obtained with far fewer integration steps. In the principal calculations we used a basis of 161 eigenfunctions $|\phi_n\rangle$ ($n_{\max} = 80$). The additional simulations with significantly smaller and larger basis were carried out to test the convergence of the integration scheme.

[1] M. Davis and E.J. Heller, J. Chem. Phys. **75**, 1 (1981).
[2] W.A. Lin and L.E. Ballentine, Phys. Rev. Lett. **65**, 2927 (1990).
[3] W.A. Lin and L.E. Ballentine, Phys. Rev. **A 45**, 3637 (1992).
[4] A. Peres, Phys. Rev. Lett. **67**, 158 (1991).
[5] J. Plata and J.M. Gomez Llorente, J.Phys. **A 25**, L303 (1992).
[6] F. Grossmann, T. Dittrich, P. Jung, and P. Hänggi, Phys. Rev. Lett. **67**, 516 (1991).
[7] F. Grossmann, P. Jung, T. Dittrich, and P. Hänggi, Z. Phys. B **84**, 315 (1991).
[8] F. Grossmann, T. Dittrich, and P. Hänggi, Physica B **175**, 293 (1991).
[9] T. Dittrich, F. Grossmann, P. Jung, B. Oelschlagel, and P. Hänggi, Physica A **194**, 173 (1993).
[10] R. Utermann, T. Dittrich, and P. Hänggi, Phys. Rev. E **49**, 273 (1994).
[11] R. Roncaglia, L. Bonci, F.M. Izrailev, B.J. West, and P. Grigolini (unpublished).
[12] M. Wilkinson, Physica **21D**, 341 (1986).
[13] M. Wilkinson, J. Phys. A **20**, 635 (1987).
[14] O. Bohigas, S. Tomsovic, and D. Ullmo, Phys. Rep. **223**, 43 (1993).
[15] M. Latka, P. Grigolini, and B.J. West, Phys. Rev. E **50**, 596 (1994).
[16] G.M. Zaslavsky, R.Z. Sagdeev, D.A. Usikov, and A.A. Chernikov, *Weak Chaos and Quasi-regular Patterns* (Cambridge University Press, Cambridge, 1991).
[17] A.W. Chao *et al.*, Phys. Rev. Lett. **61**, 2752 (1988).
[18] G.P. Tsironis, Accelerator Physics Notes, Fermi Labs Report No. 90-001, 1990 (unpublished).
[19] S.B. Lee and M.D. Feit, Phys. Rev. E **47**, 4552 (1993).
[20] S. Chu, Adv. Chem. Phys., **73**, 739 (1989).
[21] M. Hillery, R. F. O'Connell, M. O. Scully, and E. P. Wigner, Phys. Rep. **106**, 122 (1984).
[22] K. Husimi, Proc. Phys. Math. Soc. Jpn. **22**, 264 (1946).
[23] K. Takahashi, Prog. Theor. Phys. Supp. **98**, 109 (1989).
[24] M.J. Stevens and B. Sundaram, Phys. Rev. A **39**, 2862 (1989).
[25] A.K. Rajagopal, Phys. Rev. A **27**, 558 (1983).
[26] L.D. Landau and E.M. Lifshitz, *Quantum Mechanics* (Pergamon, Oxford, 1958).
[27] C. Cohen-Tannoudji, B. Diu, and F. Laloe, *Quantum Mechanics* (Hermann, Paris, 1977).
[28] T. Geisel, G. Radon, and J. Rubner, Phys. Rev. Lett. **57**, 2883 (1986).
[29] G. Radon, T. Geisel, and J. Rubner, Adv. Chem. Phys. **73**, 891 (1989).
[30] L.E. Reichl, *The Transition to Chaos* (Springer-Verlag, New York, 1991).
[31] M. Toda and K. Ikeda, J. Phys. A **20**, 3833 (1987).
[32] R.V. Jensen, S.M. Susskind, and M.M. Sanders, Phys. Rep. **201**, 1 (1991).
[33] H.P. Breuer and M. Holthaus, Ann. Phys. (N.Y.) **211**, 249 (1991).
[34] J. Henkel and M. Holthaus, Phys. Rev. A **45**, 1978 (1992).
[35] M. Latka, P. Grigolini, and B.J. West, Phys. Rev. A **47**, 4649 (1993).
[36] K. Leo, J. Shah, E.O. Gobel, T.C. Damen, S. Schmitt-Rink, W. Schafer, and K. Kohler, Phys. Rev. Lett. **66**, 201 (1991).
[37] M. Latka, B.J. West, and P. Grigolini (unpublished).
[38] M. Kac, Am. Math. Monthly **73**, 1 (1966).
[39] G. Casati, B.B. Chirikov, D.L. Shepelyansky, and I. Guarneri, Phys. Rep. **154**, 77 (1987).

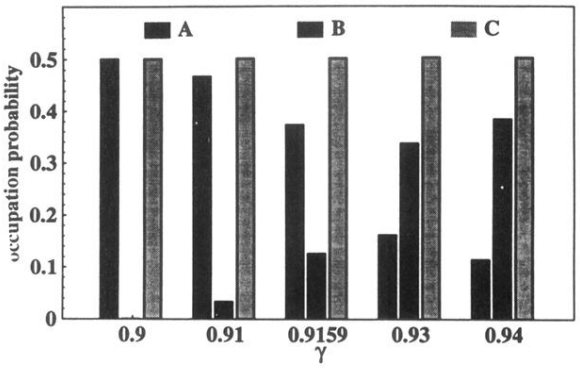

FIG. 10. Expansion of the wave packet from Fig. 8 in the Floquet basis determined for different values of the amplitude γ.

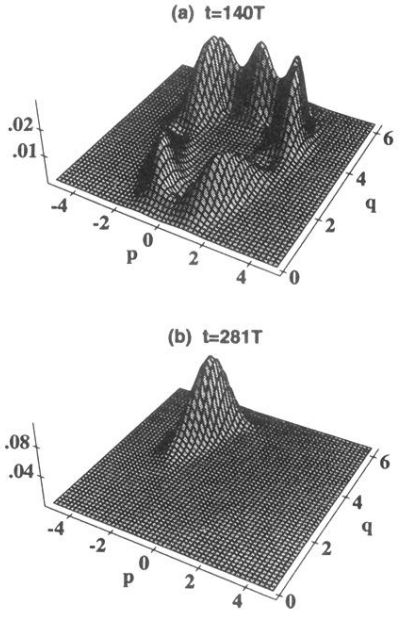

FIG. 12. Husimi representation of the wave packet in the numerical experiment from Fig. 11(b) calculated at (a) $t = 140T$ and (b) $t = 281T$.

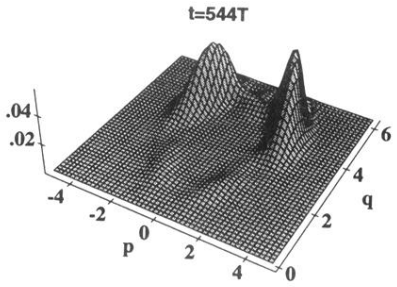

FIG. 13. Husimi representation of the wave packet in the numerical experiment from Fig. 11(d) calculated at $t = 544T$.

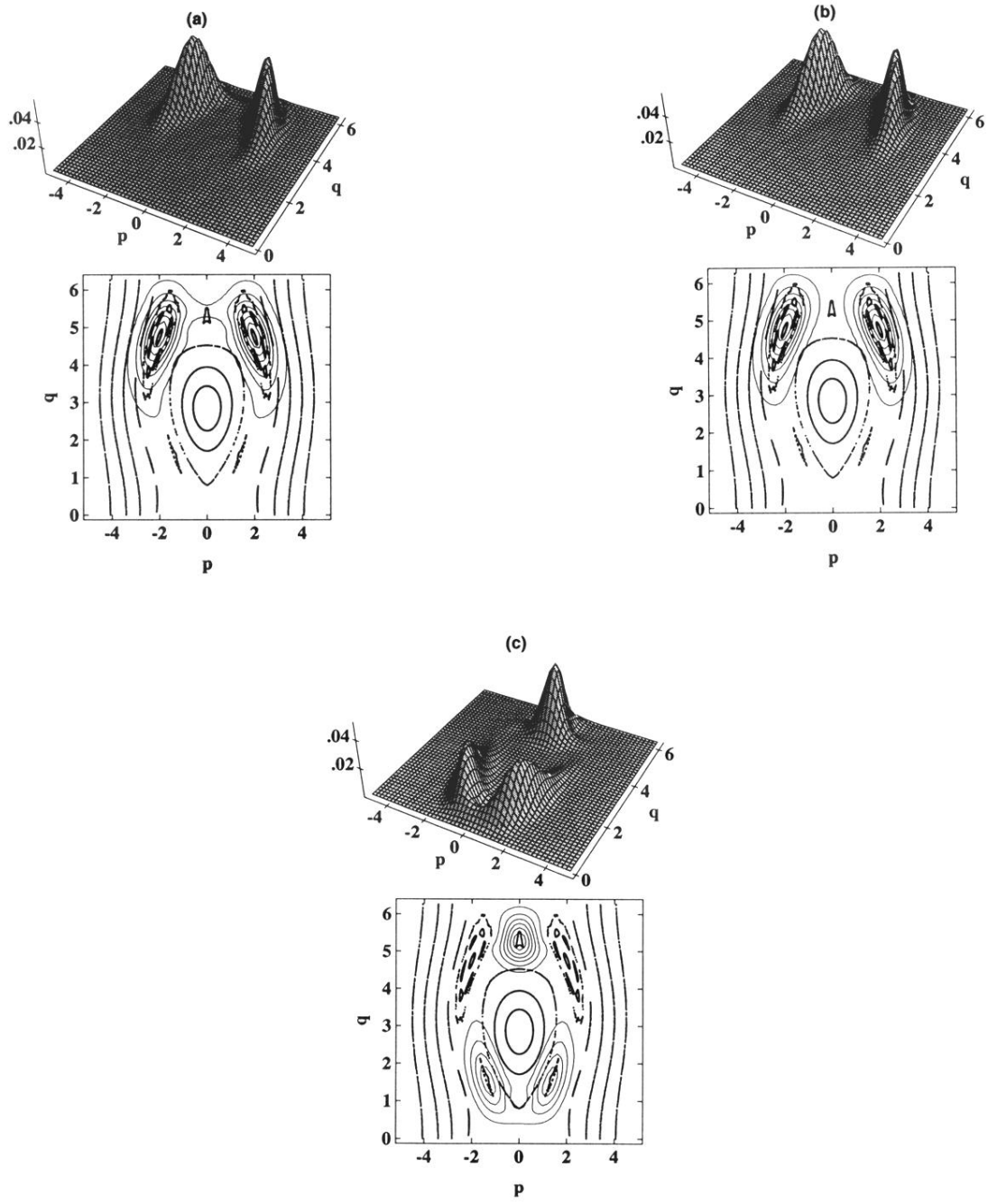

FIG. 4. Husimi representation of the Floquet states shown in Fig. 1(b). Momentum was scaled by the parameter μ. The model parameters are the same as in Fig. 2. (a) corresponds to quasienergy state A, (b) to state C, and (c) to B.

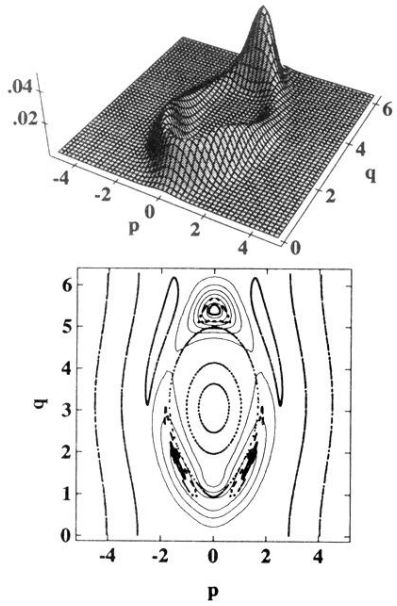

FIG. 5. Husimi representation of the Floquet state B for the small value of the amplitude of the driving force $\gamma = 0.25$. Momentum was scaled by the parameter μ. Notice the much larger size of the nonlinear resonance which underlines the structure of this state.

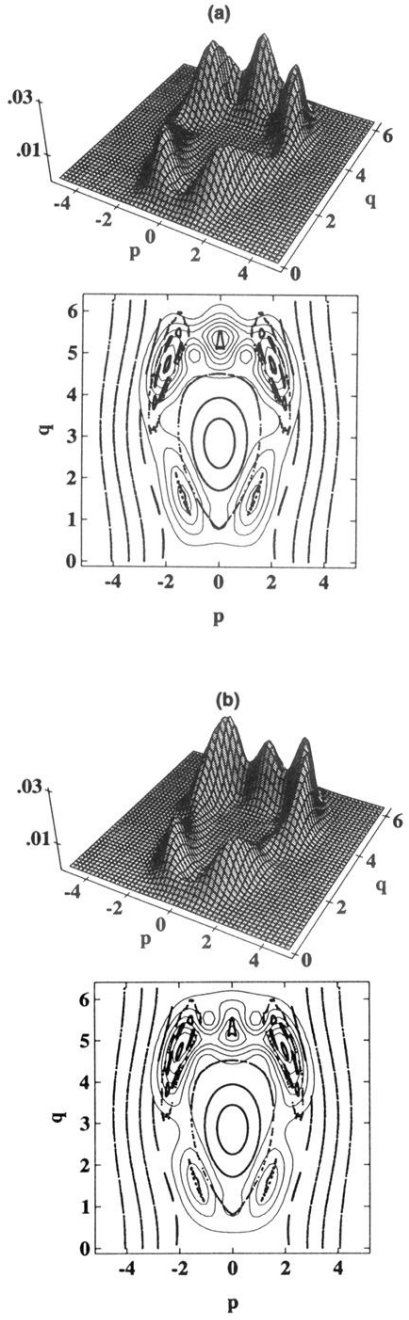

FIG. 7. Husimi representation of the Floquet states shown in Fig. 1(b) at the center of the avoided crossing. Momentum was scaled by the parameter μ. (a) corresponds to quasienergy state A, (b) to B.

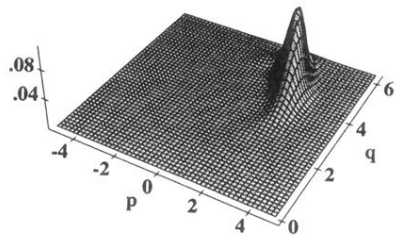

FIG. 8. Husimi representation of the symmetric combination of the quasienergy states A and C calculated for $\gamma = 0.90$.